

5 Assembly

5.1 Introduction

The previous chapter discussed the fabrication of polymer film heat transfer elements (HTE's). This chapter deals with the assembly of such air mattress shaped elements to form a heat transfer unit. This unit is inserted and suitably mounted into the larger, lower compartment of a vertical vacuum vessel which has a turbo centrifugal vapour compressor in the upper compartment.

The vacuum vessel and its auxiliary water pumps, feedwater heater, vacuum pump with protecting condenser, high speed rotary vacuum seal and (ceramic) bearings for the compressor, with valves, windows . . . form the desalinator. They are described in this chapter.

5.2 Heat Transfer Unit

A heat transfer module for the desalinator comprises welded air mattress-like plastic films joined together in a single unit with 3 manifolds:– for vapour inlet, saline water distribution, and distillate collection. After ambitious, expensive and time-consuming earlier trials attempting to manifold smaller diameter air mattress-like elements, we decided to build up the vapour inlet manifold - for introducing compressed vapour into the air mattress shaped heat transfer elements for condensation - of pieces as shown in plan in figure 5.1a. The weld line parts of the heat transfer elements are clamped between the short straight line sections of adjacent elements. To avoid the flow resistance on entry due to the *vena contracta* phenomenon, it was decided to round the entry ports. Thus a side view of an entry hole appears as in figure 5.1b [2,3]. This is built into the shape of the manifold pieces, of which 5.1b is therefore an illustration.

Initially the idea was to drape the welded film over the top of the manifold pieces, and to use smaller diameter film tubes. Manifold pieces designed with this in mind are shown in figures 5.2a-d, and were made directly from electronic versions of our 3 dimensional CAD (computer aided drawing) drawings.

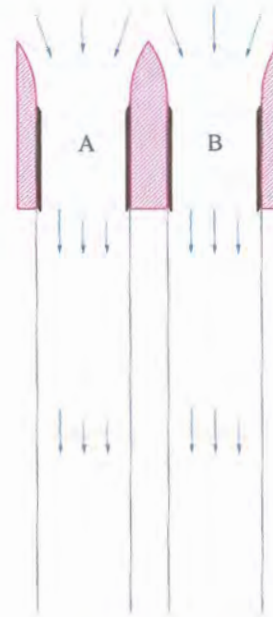
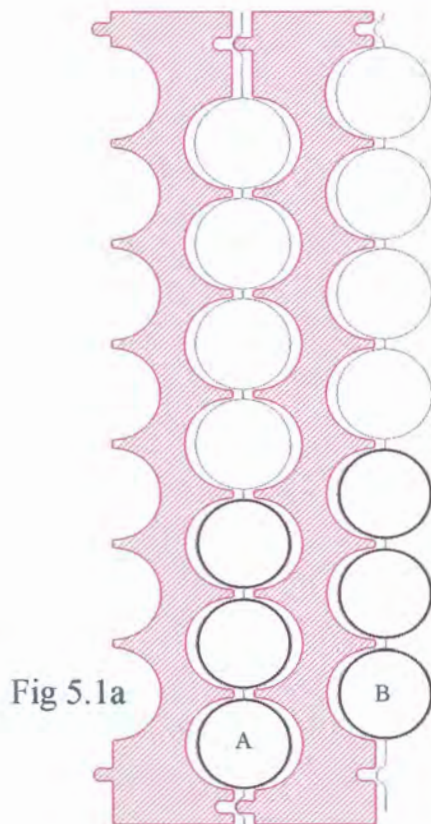


Fig. 5.1 (a) Top view of part of a manifold, showing air mattress shaped film elements (thin blue lines) to be clamped between manifold pieces. The lowermost 3 film tubes also show short thin-walled tubular inserts (thicker black lines) that will press them against the manifold pieces when these are clamped. The friction of this clamping and pressing is what hold the film elements in place. (b) Side view of entry ports into adjacent film tubes like A and B (see fig 5.1a). The entry flow paths are rounded to avoid *vena contracta* type flow resistance. The thin-walled closely fitting tubular inserts – with one end tapered to facilitate insertion – offer only a minimal flow resistance.

[We used Allicad for 2 dimensional, and Solid Works for 3D drawings]. The pieces were for HTE's with 40 polymer film tubes of 4mm diameter. This version was manufactured by a stereo lithography process. Despite the poor results from this process at the required high resolution, they clearly showed that (even if the parts had been manufactured perfectly), the relatively stiff 50 μ welded polypropylene film would not drape as desired over the top of the finely sculpted three dimensional manifolds.

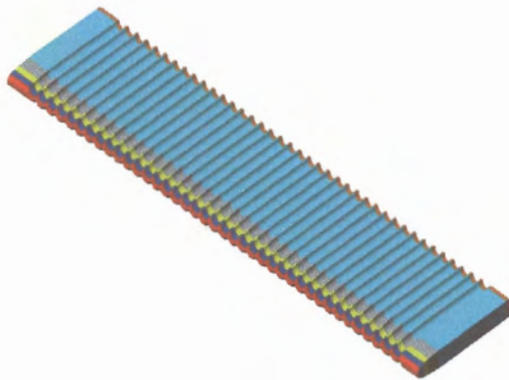


Fig. 5.2a

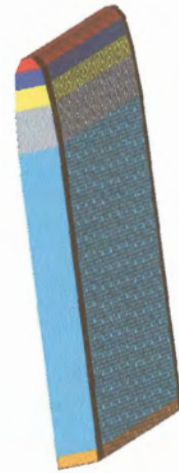


Fig. 5.2b

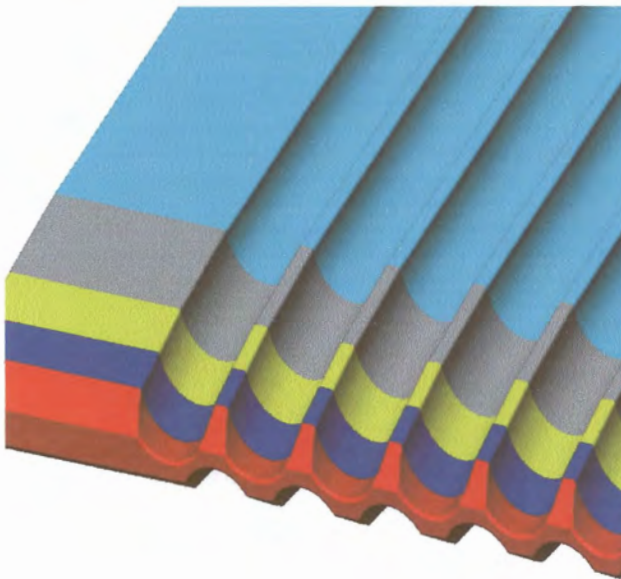


Fig. 5.2c

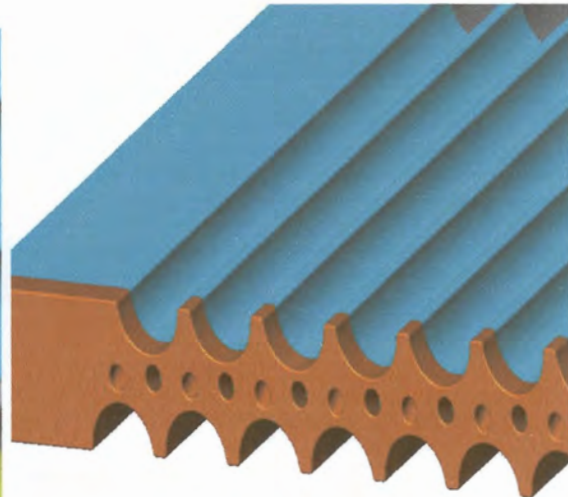


Fig. 5.2d

Fig 5.2 Initial design for a vapour manifold piece – intended for use with 4mm diameter polymer film tubes:– (a) isometric view; (b) side view; (c) close-up top view; (d) close-up bottom view, showing the small holes for distributing saline water to each individual film tube on each side of this part, which was also intended to serve as saline water distributor. The saline flow per hole would, however, be so low that blockages due to dirt particles or scale would be likely.

Therefore a HTE with seven film tubes of 18.4mm diameter was designed and fabricated, along with new vapour manifold pieces (see figure 5.1) to fit them. Instead of trying to drape the film over the top of the manifold pieces, we had thin walled tubular pieces made to tightly fit into the upper parts (the *necks*) of the film tubes, to hold the tube entrances open. Also - by pressing them onto the concave semi-cylindrical parts of the manifold pieces - to help hold them by friction.

Figures 5.3 a - b show an assembled vapour manifold.

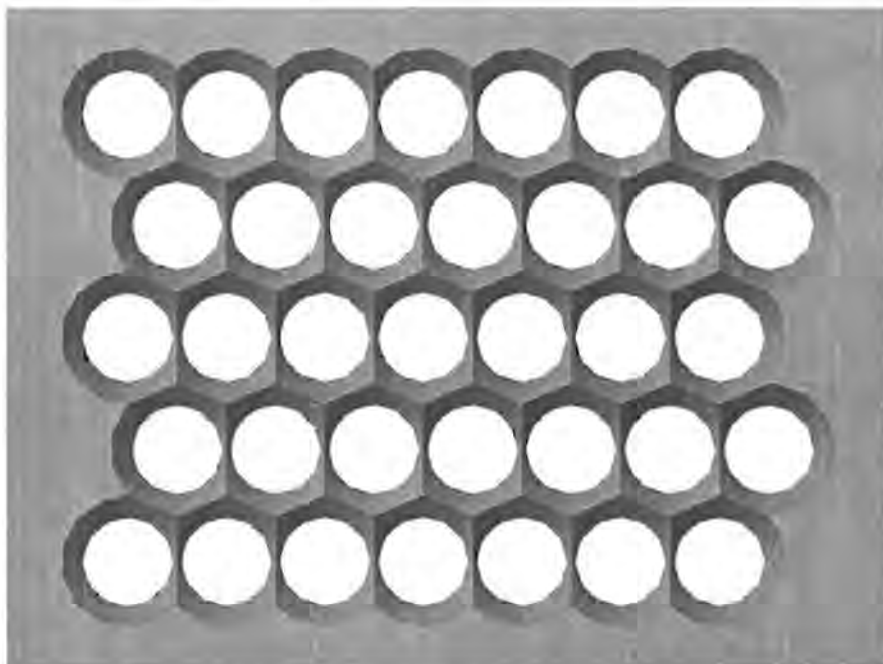


Fig 5.3a Vapour manifold entry for 35 film tubes of 18.4mm diameter, with rounded (*anti-vena contracta*) inlets as shown in fig 5.1b.

The insertion of the thin-walled tubes into the films requires care to avoid damaging the films. In order to obtain the necessary tight fit – and to establish which insert diameter would give the best round shape in the tubes of the HTE – thin walled tubes of outside diameters 18.1, 18.2, 18.3 and 18.4mm were separately inserted inside each tube of a HTE. The manifold pieces were then clamped on. The tests indicated that the 18.1mm inserts – apart from being easiest to insert, and having the smallest risk of damaging of the film tubes – also gave the roundest film tubes on assembly with the PP HTE's.

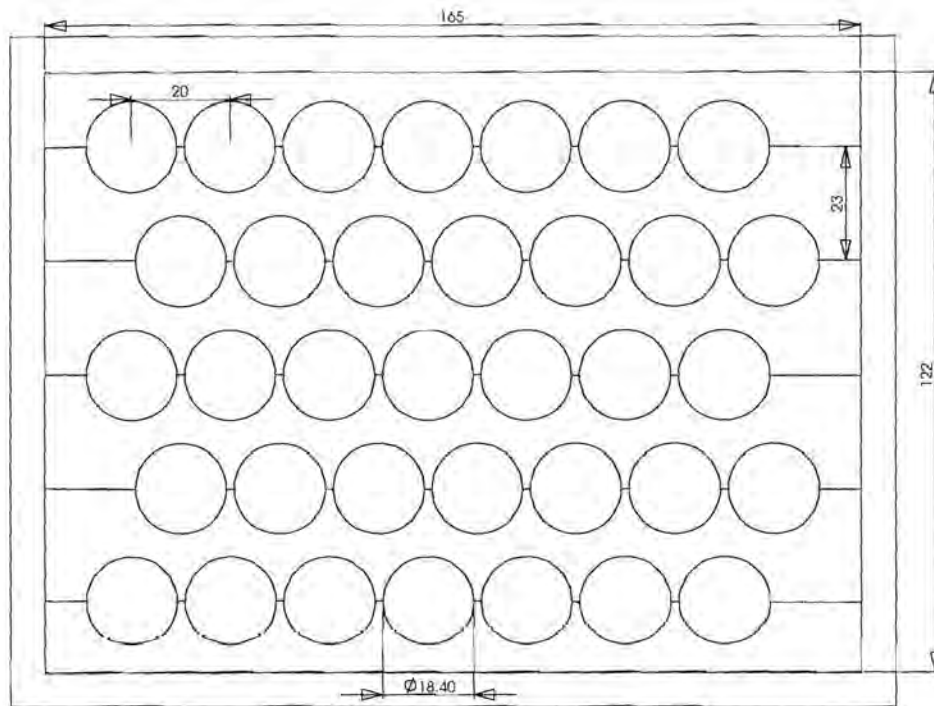


Fig.5.3 b Top view of a manifold with some relevant dimensions in mm.

The heat transfer unit comprises 70 tubes of 18.4mm diameter and 2m long. This corresponds to a surface area of 8m^2 . At the top, the heat transfer unit is fixed on a plate separating the 2 vacuum compartments through two vapour manifolds. At the bottom, each “air mattress” is connected through a small tube to a main plastic tube – the liquid collecting manifold – that is used to collect the distillate before it is pumped from the vacuum vessel.

5.3 Vacuum Vessel

The vacuum vessel was manufactured by an engineering company specializing in borehole casings, from 3mm thick mild steel reinforced with 20mm thick external circumferential ribs at 660mm intervals. Top and bottom plates are also of 20mm steel. It has an inside diameter of 400mm and a total height of 2310 mm, and is shown in figure 5.4. It has a main compartment (everything up to the flange about 290mm from the top), and an upper one which houses the vapour compressor.



Fig 5.4 The uninsulated 2.35m tall vacuum vessel showing 200mm windows, stand and scaffolding. The pulley block is used to raise and lower the small top compartment (housing the turbo centrifugal compressor, and at a pressure $p + \Delta p$ above that of the main compartment).

The upper compartment is at the increased pressure $p + \Delta p$ of the compressor outlet. Between the main and the top compartments is a removable separator plate of 15mm polypropylene, which has at its centre a suction port leading to the centrifugal compressor inlet.

The main compartment has five windows, and a removable bottom lid, and is held by the stand and scaffolding. The windows - three of 200 mm and two of 160 mm diameter - are

to enable one to check on the wetting of the polymer heat transfer elements. They also facilitate access to the inside. In operation the windows have 6 mm thick heat toughened glass disks - 165 mm diameter for the small and 204 mm for the big windows. The bottom small window is now sealed with a stainless steel disk with a vacuum hose connector – to couple the vessel to the vacuum pump.

The separator plate separates two regions of different pressures: p in the main compartment, where evaporation takes place *outside* the film tubes, and $p + \Delta p$ in the upper compartment, which contains manifolds leading to the *inside* of the film tubes. Figure 5.5 shows a bottom view of the configuration adopted. Below the separator plate, a plastic tube extending from outside the vessel, is used as inlet for saline water. The tube is connected through a T-junction to a series of multiply drilled small tubes (liquid distributors) placed between adjacent air mattresses-like HTE's, with enough holes to wet each film tube on each side of each small tube with an even film of saline water. Thus each small tube acts as a saline water distributing manifold, which is further equipped as detailed in Chapter 6.

To prevent corrosion of the vessel, two coats of a phenolic epoxy tar coating (TCN300) were applied directly to the cleaned, sandblasted carbon steel. The coating took weeks to harden – into an uneven surface resembling a tarred road.

Vacuum seal. The flange sealing surfaces and O-ring grooves were distorted by the welding process, and needed re-surfacing – on a huge lathe bigger than that of the manufacturer. These surfaces were then painted with a marine epoxy (Copon) which hardened within an hour or so into a smooth hard surface more suitable for vacuum sealing. But even now (at least one of) the many seals (5 windows, 415mm diameter bottom seal, 2 seals of 415mm diameter at the separator plate, plus many smaller diameter seals) are far from satisfactory. It would have been much better to require from the manufacturer a pre-test and guarantee of the seal - even if this had more than doubled the cost of the vessel. Perhaps at least the *sealing surfaces* should also have been of 304 or 316 *stainless steel*.

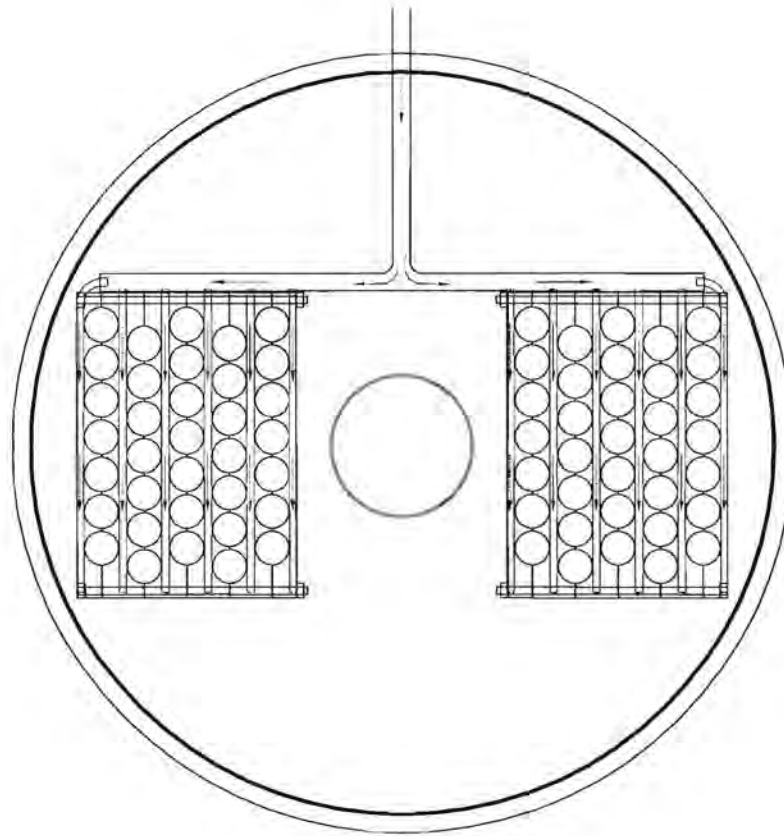


Fig. 5.5 Schematic bottom view of the separator plate with the water inlet and the liquid distributors tubes. Two manifolds used to join the air mattresses (five each) are presented. The evaporating vapour reaches the compressor through the orifice (circle) at the centre of the plate.

5.4 System Auxiliaries

The auxiliary components connected to the vacuum vessel include a vacuum pump, water pumps, a turbo centrifugal vapour compressor, a specially made water cooled high speed rotary vacuum seal, specially made (in Germany) high speed bearings (with ceramic balls), a small plate heat exchanger, feedwater heater, and measuring instruments.

5.4.1 Vacuum Pump

Two types of vacuum pump were tested. The first pump was a small plastic ejector type water jet pump. Due to the low pressure of the water supply it evacuates the vessel too slowly – even when connected to two water taps in parallel. It can of course not achieve

the desired absolute pressure of 1 mbar under dry conditions that we deem necessary as indicator of an adequate vacuum seal (zero infiltration of unwanted non-condensable gases).

The other pump is an oil-type vacuum pump (LH – Leybold – Heraeus, Trivac, D16A). This evacuates the vessel faster, and to absolute pressures of about 1 mbar when dry.

5.4.2 Water Pumps

In the system three water pumps are employed. One is used to maintain continuous circulation of ice water through the small **plate heat exchanger** used as a **condenser** to trap the water vapour evacuated from the vacuum vessel – preventing it from reaching the vacuum pump. For removing the distillate and the concentrate brine from the vacuum vessel, and re-circulating part of the brine, two air-operated double-diaphragm pumps (Wilden P.025) were employed – with all wetted solid parts of polypropylene [1].

Unfortunately the diaphragm pumps – located on the floor below the desalinator – are unable to retrieve the distillate and the brine from the vacuum system when the absolute pressure in the latter is below 10 kPa. This is despite the claim [1] that it is “capable of pulling a high vacuum”. Thus we built an apparatus based on a barometric principle to extract these by gravity. Unfortunately this is somewhat inconvenient, as the distillate is now collected 4 stories (12 m) below the apparatus. And the barometric pump needs careful priming and (like everything else) air-tight seals. And staff at widely different levels.

5.4.3 Centrifugal Vapour Compressor

The specially designed and built centrifugal turbo compressor is mounted inside the small upper compartment. It is driven by a shaft passing through a rotary vacuum seal cooled and sealed with a trickle of water. As the seal is just a millimetre below a specially made imported bearing, it must be carefully wetted – and the surplus water continuously removed by suction – to keep the expensive bearing dry. A special grooved high speed drive belt passes over a 210 mm pulley mounted on the shaft of a 3 kW, 2 900 r p m electric motor, and drives a 30 mm pulley on the impeller shaft at about 20 000 r p m.



Fig 5.6 Upper part of the vacuum vessel with the motor for the compressor. The inverted orientation of the motor is to get the correct sense of rotation of the impeller.

See figure 5.6. [Initially we had bought a 2.2 kW industrial router – with 12.7 collet chuck and the valuable feature of a *speed controllable from 9 000 to 27 00 r p m*. Unfortunately all routers rotate in the same sense (direction) – the opposite of that of all readily available impellers for turbo machinery. And the bearing of the router appeared incapable of safely supporting even the dynamically balanced 127 mm diameter impeller at speeds much above 12 000 r p m. Fortunately, we were able to return the router for a full refund a few days after buying it. But the change caused a huge delay, as the compressor needed modification. In all, it took more than 2 years to get the compressor operational, as the manufacturer had another project (a gyrocopter) of higher priority to it.]

The compressor was designed for a low compression ratio (1.02 - 1.04) to give a small temperature difference (below 2°C) in the evaporator/condenser.

5.4.4 Measuring Devices

The pressure in the main compartment is measured with a simple Bourdon type gauge giving the pressure relative to atmospheric on a scale 0 to -100 kPa. When testing the vacuum sealing, a gauge giving the *absolute* pressure on a scale 0 - 25 mbar (0 - 2.5 kPa) is used.

When the compressor is running, the pressure difference between the compartments is measured by a (coloured) **water manometer**. We found, to our surprise, that the initial manometer gave a non-zero reading when both sides were at equal pressure – even when both were open at atmospheric pressure! The cause was capillary effects and different surface tension of the glass on the 2 sides – induced during the heated bending of the tube. No amount of ultrasonic detergent cleaning would remove this – the only solution was to have a U bent out of much larger diameter glass tubing.

The feed water flow rate is measured with a calibrated 1/4 inch Fisher and Porter rotameter. This was calibrated using a stopwatch and large measuring cylinder. The feed water is supplied from a big tub. A glass thermometer indicates the temperature of water from the **specially built flow-through feed water heater**. Flow into the desalinator is regulated by a valve, and the heating power by a variable transformer. For a *laboratory* MVCD heat recovery flat plate heat exchangers to recover heat from the brine and distillate streams (to pre-heat the feed) was not deemed necessary or cost-effective.

Our experience suggests that a *heating element* in the brine at the bottom of the desalinator would be useful – to speed the warm-up of the apparatus from a cold start. It could be switched on even before the vacuum pump (which needs circulating ice water to protect it) – to warm the apparatus by condensation of water vapour from the warmed water.

5.5 Experimental Procedure

The schematic setup of the vertical vapour compression desalinator designed to operate between 50 and 65°C is shown in figure 5.7. In this temperature range the scaling potential is very low for seawater and for most industrial effluents. Although scale does not adhere to untreated non-polar polyolefin surfaces, it is expected to adhere to some

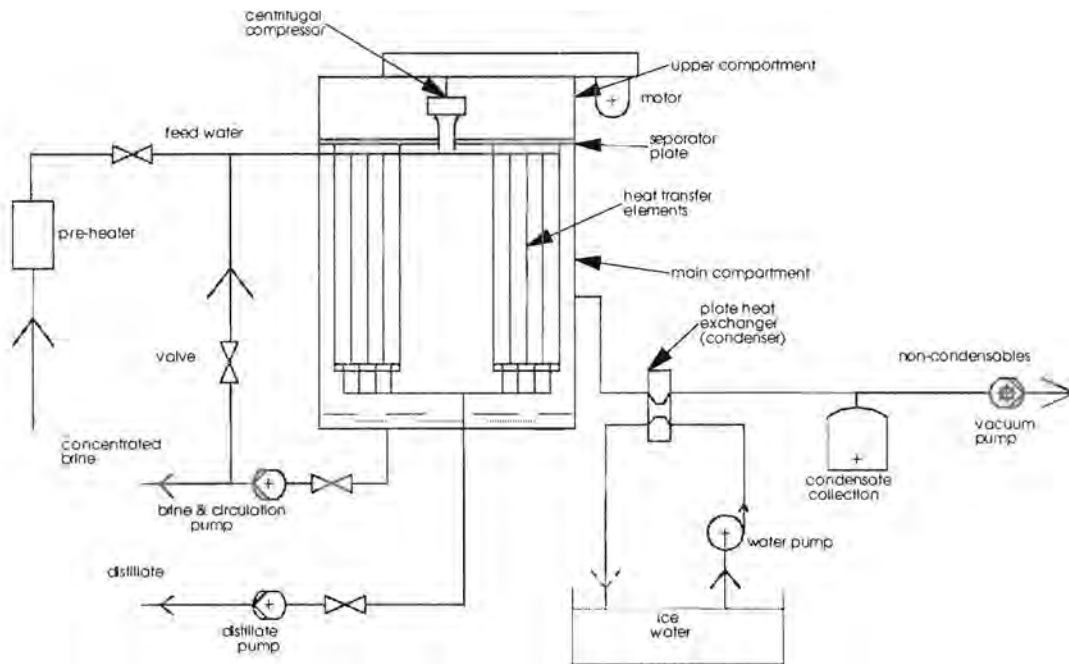


Fig. 5.7 Schematic diagram of the desalinator with auxiliaries.

extent to surfaces treated for wettability – see chapter 6. This treatment is needed in order to utilize film-wise evaporation. The evaporator-condenser has vertical air mattress-shaped HTE's joined together as described in section 5.2. Until now, the testing of the desalinator has started with the evacuation of the vessel under *dry* conditions. This was to test the overall tightness of the various vacuum seals, which needed to be covered with silicone sealer to make them effective. At an initial absolute pressure of about 1 kPa pre-heated feed water is drawn into the vessel. Inside, the feed water is dispersed over the outer surface of the plastic film tubes through the saline water distributors. A small part of the water moving downwards evaporates. For efficient evaporation – due to transfer of latent heat of condensing vapour inside the HTE's – it *should flow down as a film* to the bottom of the vessel from where it is pumped out of the evacuated apparatus. Part is discharged, and part recirculated with the pre-heated feed.

The vapour from the evaporated liquid is drawn into the compressor. By increasing the

pressure the compressor raises the saturation temperature (at which the vapour condenses). Compressed vapour flows via the manifolds into the film tubes. There it condenses releasing latent heat which is transferred through the tube walls to evaporate feed water flowing on the outside surface of the plastic films. Thus, additional vapour is produced and the process repeats itself again and again. However, the saline water *did not actually flow down the HTE's as a film*. In the time it took for the silicone sealer to dry (several days inside the “crevices” between mating surfaces), the film elements dried out, and their wettability was irreversibly reduced – see chapter 6. The result was that – as far as could be judged by looking through the windows – **only about 5 - 10% of the film heat transfer surface was wetted**. Water was seen to be dripping and running in narrow streamlets – instead of flowing filmwise. Thus it is no surprise that the performance of the apparatus (as judged by the amount of distillate formed inside the HTE's) was disappointing.

5.6 Recommendations

An alternative procedure would be to put several centimetres of water in the bottom of the apparatus once the bottom plate is in position with its bolts tightened. The pump for recirculating this water to the top of the HTE's is then “switched” on (by opening a valve for compressed air) in order to (try to) keep the HTE's wet. One proceeds to tighten all other apertures and connections, and carefully applies silicone sealant to all of these. After about 24 hours the heating element inside is switched on to speed up the curing of the sealant. The interior is kept at about 60°C for the following 24 hours to complete the curing process. With the apparatus already warmed up, it could be evacuated and started up fairly quickly.

However, there is some doubt as to how successful this would be. Even the day or so of dryness needed to assemble new HTE's into the apparatus with also the distillate collecting manifold in some difficult-to-reach positions (and tightening all the seals) can affect their wettability. Pumping water onto the already dry HTE's will not wet more than about 30% of their surface. Merely bolting on the bottom might be insufficient, as its 415mm diameter seal might leak. And the procedure does not allow one to test the

tightness of the vacuum seals, which requires dry conditions.

What is really needed is a laboratory apparatus:–

- (a) that permits *inspection during operation* of the *full* heat transfer surface of *at least* one HTE to check the wetting. This is essential before any measurements or optimization of the key parameter U can be made – or even seriously contemplated. Optimizing the heat transfer coefficient U is a key to any serious design of a new type of desalinator [4]. This feature is also needed for studying how scale is formed from highly concentrated industrial wastes, and what surface treatments will lead to good wetting, but avoid or minimize scale adhesion.
- (b) that can be made vacuum tight in minutes – not days;
- (c) where the HTE's can be easily flooded over their entire external surface *after closing the apparatus*; or
- (d) where they can be assembled (and the apparatus closed) *before drying out*.

In a production apparatus, requirement (c) (if needed together with (d):– keeping the HTE's wet before & during installation) will be a key to success. This is impossible to attain in a vertical setup, but rather easy in a **horizontal tube configuration**. Furthermore, recent work has shown that a horizontal system – which is outside the scope of this thesis – also leads to simpler, less expensive HTE's, to much improved wetting, and to far simpler (spray type) saline water distribution.

Indeed it will have about a *thousand times fewer water distributors* (now of the full bore type, rather than the more easily clogging capillary type used for the vertical configuration). These are of critical importance [5] as they

- (A) can clog;
- (B) need to be monitored; and
- (C) when blocked, must be promptly and quickly replaced without cooling down the

apparatus.

If requirements (B) and (C) are not met, irreversible damage will result to the HTE's, which will dry out in parts, and may lose their wettability or scale up.

5.7 Summary

The assembly of the air mattress-like heat transfer elements (HTE's) using the adopted manifold pieces to build a single heat transfer unit was successfully accomplished. Also specifying, obtaining, installing (and where needed, designing and constructing) the various auxiliaries.

Although this would have at least doubled the cost of the vacuum vessel, it would have been much better to have required the contractor who built it to have pre-tested it against leaks, and to give a guarantee on this. Perhaps also the sealing surfaces should have been of stainless steel. The use of silicone to improve the sealing of vacuum vessel - to prevent leakages - was labourious.

A laboratory polymer film apparatus should satisfy the requirements (a) - (c) – or (a), (b) & (d) – of the previous section. A production desalinator should at least satisfy the key requirement (c) – as well as requirements (B) and (C). These requirements can only be met (at affordable cost) in a *horizontal* (film) tube desalinator.

5.8 References

1. “*Engineering Operation and Maintenance*”, Wilden technical manual, EOM-P.025P 8/00.
2. J. Bijkersma, *Pressure losses at the tubular inlet section of a low temperature differential heat exchanger*, M Eng thesis, RAU, 2003.
3. J. Bijkersma and L. Pretorius, *Design parameters to minimize pressure loss for an axisymmetric inlet section evaluated*, 3rd International Conference on Heat Transfer, Fluid Mechanics, and Thermodynamics, Cape Town, South Africa, 2004.

Also (same title) J. Bijkersma, L. Pretorius and J. P. Meyer, SACAM Conference,

Johannesburg, South Africa, 21-23 January, 2004.

4. E. Ghiazza and P. Peluffo, *A new design approach to reduce water cost in MSF Evaporators*, Proceedings of IDA conference, Paradise Island, Bahamas, 2003.
5. V. Baujat and T. Bukato, *Research and development towards the increase of MED units capacity*, Proceedings of IDA conference, Paradise Island, Bahamas, 2003.

6 Wettability and Wetting

6.1 Introduction

6.1.1 Efficient Evaporation

Pool boiling (used in older, pre-1950 multi-effect stills) is inefficient at low ΔT_e , as both the static pressure head and the considerable pressure effects of surface tension on the formation of tiny steam bubbles must be overcome. *Falling film evaporation* is used in all modern multi-effect (ME) and vapour compression (VC) desalinators.

The *falling film* refers to a thin film of saline *water* trickling ("falling") down a heat transfer surface - whether this be a metal tube or a polymer film heat transfer element. A falling film evaporator presents a large surface area for evaporation, and a heat transfer coefficient h_e for evaporation that (in the Nusselt theory) *increases* as ΔT_e decreases. It is thus particularly suitable for high efficiency stills, which require small ΔT_o and hence even smaller ΔT_e .

Efficient, i.e. falling film evaporation requires that the evaporation surface of the polymer heat transfer element be thoroughly *wettable - hydrophilic*. A thin, preferably uniform and continuous water film should flow downwards on the heat transfer surface.

The most efficient condensation, by contrast, is dropwise condensation, [1,2,3] which needs a *hydrophobic* - water repellent - surface. Therefore the ideal is a surface that is strongly hydrophilic (water attracting, and therefore wettable) on the evaporating side, but strongly hydrophobic on the condensing side.

6.1.2 Surface Modification

It is well known that the polar liquid water does not wet polyolefins, which are non-polar and mildly hydrophobic. This is due to the low surface tension of polyolefins (~ 30 mN/m) compared to water (~ 70 mN/m). The surface tension and wettability of a polyolefin surface can be increased by subjecting it to a suitable surface treatment. Possible chemical surface treatments include exposure to corona discharge, to gaseous ozone (O_3), to gaseous SO_3 , to oleum, to chromic acid, to sulfamic acid, and

oxyfluorination. During oxyfluorination the polyolefin surface is exposed to a fluorine - oxygen - nitrogen gas mixture. This results in functionalization of the surface: charged, dipolar and/or polarizable sites are created. All of these tend to increase the affinity for water, which comprises dipolar molecules.

Wettability is a material property while wetting depends on the wettability and on the recent - *temporary* - history of the hysteresis of the material.

6.1.3 Unwanted Capillary Action

Once the evaporating outer surface has been made wettable, an unwanted capillary action arises in the space between adjacent film tubes: Saline water flowing down the outside of the set of tubes tends to move to the region where the weld line separates adjacent tubes (see figure 6.1). This depletes and/or removes the water film from the rest of the surface. Thus it can happen that most or all of the water eventually flows along the weld lines - where little heat exchange can take place between condensation inside and evaporation outside - leaving the regions where evaporation *should* take place dry. Such large dry areas are unacceptable [10]: in the process of drying out they can form *scale*, and, once dry, they do not contribute to the evaporation.

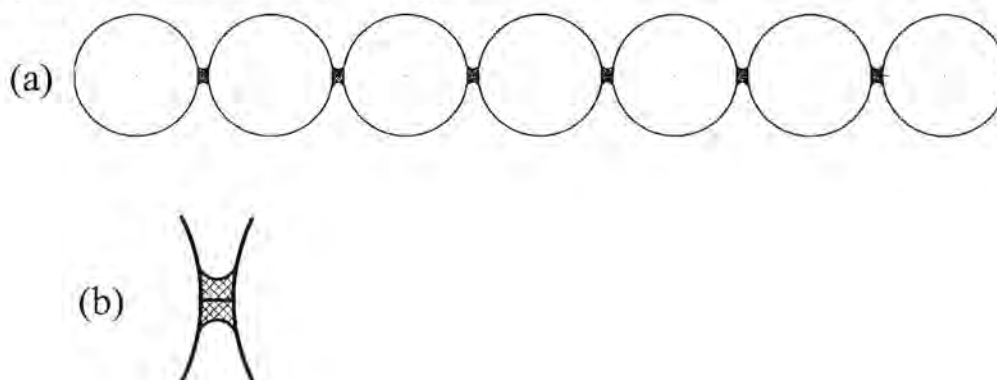


Fig.6.1 (a) Capillary action between adjacent film tubes, in the region of the weld lines, between adjacent film tubes (b) a close-up view of the capillary zone. In our test setup, each “air mattress” has seven film tubes. Water is drawn into the region between adjacent tubes - that is, into the film region nearest to the weld lines.

As side-wise conduction will be minimal in a thin ($\sim 30\mu$) polymer film (with low conductivity $k \approx 0.2$ to 0.4 W/mK), the condensation directly opposite to the dry areas will also cease, so that the total area for heat transmission between condensation and evaporation will be essentially the total area wetted by saline water. It was originally

thought that if the areas of the weld lines, and adjacent to them were masked (with masking or PVC tape) during the wettability treatment the natural hydrophobic character of the polymer film might be sufficient to prevent this unwanted capillary action. Unfortunately, this did not happen - most water still flowed down the vertical “furrows” between adjacent tubes. This may be for either (or a combination) of the following reasons:

- (a) The untreated polymer is perhaps not sufficiently hydrophobic.
- (b) Traces of the tape adhesive remain in the weld area after the masking/PVC tape is removed. These traces make the film somewhat hydrophilic in the very region where they are supposed to *prevent* the wettability treatment.
- (c) The masking is not sufficient to prevent some of the highly reactive chemicals to reach the region.

Another solution tried for this problem was to use spacers (see figure 6.2) that would keep the “air mattress” tubes in a constant staggered spacing relative to the tubes of the next “air mattress”. They were also designed to collect the water flowing down the “furrows” next to the weld lines, and to re-direct this water to positions halfway between “furrows”.

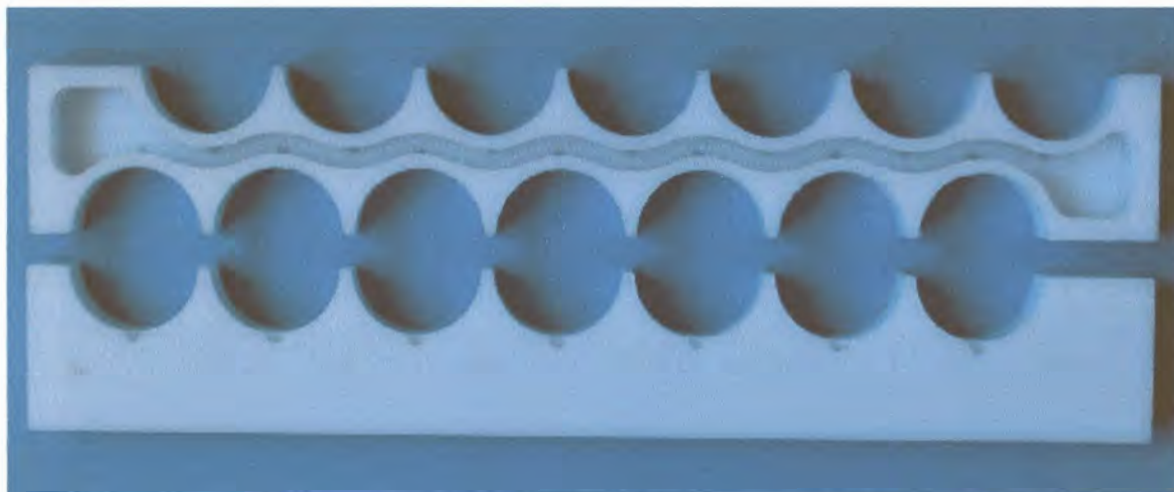


Fig.6.2 Spacers used to keep the “air mattress” tubes in a constant staggered spacing relative to the tubes of the next “air mattress”. The lower spacer is upside down.

This, too was not as successful as we had hoped. The reason appears to be that on inflating the “air mattresses”, the polymer film stretches by an amount that is difficult to

predict - as it will depend on both the pressure of inflating, and on the temperature (which strongly influences the elastic modulus of the polymer film). The “air mattresses” then no longer accurately match the dimensions of the specially made spacers. Therefore they do not effectively collect the water from the “furrows”.

By far the best solution appears to be a modification of the original - to apply a thin layer of silicone (a *strongly hydrophobic* material) to strips over and surrounding the weld lines *after* the wettability treatment (which also increases the adherability). This at present still somewhat labourious solution has proved 100% effective against the undesired capillary action. A flexible tape, adhesive on one side but strongly hydrophobic on the other, would also be effective. So far, we have not been able to find such a tape, and it is not clear whether such tape exists, or can be easily manufactured. PTFE impregnated fibre-glass cloth is available in a form that *is* adherable on one side and strongly hydrophobic on the other, but is not nearly flexible enough.

We now discuss the testing of the wettability of plastic films - to see which will be suitable for use in the still.

6.2 Wettability Test

An experimental setup used to perform the wettability tests of the oxyfluorinated “air mattress” plastic films is shown in figure 6.3. It comprises two basins, one at the bottom to collect the water and the other at a variable height and used as the water source. A flexible tube with a tap connects the top basin to two small distributor tubes (5mm ID) through a T-junction. Each distributor tube has seven holes - one at the centre of each film tube, halfway between the weld lines - to spread water evenly on the plastic films to be tested. In one distributor tube the diameter of the holes was 1.0 mm; in the other it was 1.4 mm.

Closely fitting white plastic tubes were inserted carefully (so as not to tear the thin film) inside the welded plastic film in order to attain the desired round shape for the test. The assembly of the plastic films with inserted tubes was held at the top and at the bottom.



Fig.6.3 Experimental setup for wettability test.

The figure 6.4 allows a close-up visualization of the amount of water streaming in each weld line by looking at the water level in each glass tube.



Fig. 6.4 Close-up view of the setup for separation of the fluid streams.

Figure 6.5 is a drawing of the used separation unit. The dashed lines represent the (chemical) test tubes. White silicone putty P sloping towards the apertures A was used (see figure 6.5b) to guide the flow streaming along the weld lines towards the apertures A. Each of the 6 apertures (one for each weld line *between* tubes) on one side of the air mattress had below it a test tube to collect the water streaming through that aperture. Water flowing on the air mattress surface, but not near the weld lines, would flow to be collected in the basin (outside the test tubes).

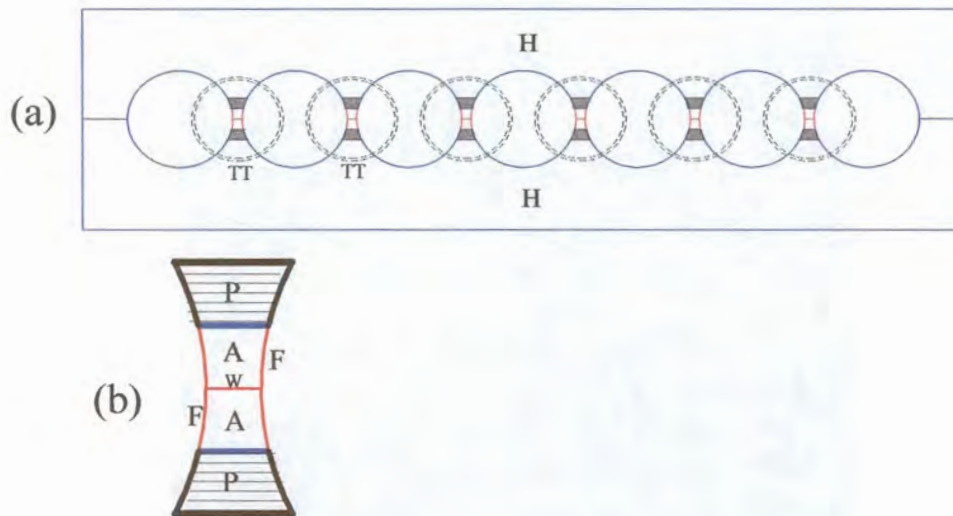


Fig.6.5 (a) Drawing of the separation unit with the white holders H and test tubes TT (dashed lines), (b) close-up view of the separation region (A= aperture, W= weld line, F= plastic film, and P= Putty).

Water from the top basin was used to wet the plastic film by letting it flow downwards at different flow rates determined by changing the height of the top basin. The water was coloured with red food colouring liquid to facilitate its visualization on the white background represented by the plastic film. A camera was used to record the images of the water flowing downwards on the welded plastic film, at different flow rates, and for different surface treatments.

The insertion of closely fitting white tubes in the “air mattress” tubes to attain the required round shape was not a suitable method for tests involving “air mattresses” of two metres long as needed for the desalinator. This procedure was abandoned in favour of one more resembling the real situation of the system in operation. Compressed air inflated the “air

mattresses”. The use of 2m long oxyfluorinated air mattresses in the wettability tests required some alterations of the experimental setup. In figure 6.6 the new setup is depicted. In this setup the top basin was removed. A small fountain pump (EDEN 130G)



Fig.6.6 Improved experimental setup for wettability test.

was employed to circulate the water from the bottom basin to the liquid distributor.

6.3 Test Results

In the first tests plain coloured water was used to wet the films, which were of bi-axially stretched polypropylene (PP). The wettability was poor. In the following tests, coloured water was mixed with a *surfactant* to reduce its surface tension. This improved the wettability. *With the new setup, no surfactant was used, as in a production desalinator it might cause environmental problems (for the brine disposal), and would also involve the cost of the surfactant. Instead every effort was made to improve the wettability of the plastic films by optimising the surface treatment process.*

The test results are presented in the following sections.

6.3.1 Test without Surfactant

From the figure 6.7, it can be seen that (red coloured) water wets the tested oxyfluorinated plastic film, but not very well.

Droplets can be observed in the picture. On each film tube a flow stream starts at the hole in the liquid distributor: half-way between the weld lines on the plastic film surface. It spreads somewhat and also meanders. Where water enters the region of the weld lines, it tends to stay there, moving vertically, and finally enters a glass tube. As seen in figure 6.4, different tubes collect different amounts of water - showing that the water flow on the plastic film is not homogeneous.

This could be because the used plastic film was not adequately oxyfluorinated (too low a treatment time, temperature or concentration). Thermodynamics suggest that it is also possible that long exposure of the treated surface (which has increased the surface tension and energy) to dry conditions *after* treatment could have caused components of the high energy surface to migrate inwards thus decreasing the charged/polar/polarizable nature of the surface, and its wettability. The exposure of a treated film to dry air for long can also cause [4,6] the lowering of the surface tension due to, for instance, absorption by the surface of low energy contaminants from the atmosphere.

6.3.2 Test with Surfactants

The results obtained in the previous experiments were not satisfactory. In the following tests, coloured water was mixed, separately, with two different surfactants (NP9 and AL2575 from Uniquema) in different concentrations to lower the surface tension of the solution. This improved the wettability of the plastic by lowering the surface energy of the water. For these tests the first setup and testing procedure was used. Five litres of coloured water were mixed with each surfactant at 10^{-5} dilution by volume. The solution was spread on the same plastic film previously used in the tests without surfactant.

The result of the first attempt was poor. Consequently the surfactant's concentration was doubled, tripled and finally kept at ten times the initial concentration. However, no satisfactory results were obtained at any of the used concentrations of either surfactant.

The use of the *same* plastic film employed in the first experiment (without surfactant) could be the reason for the poor results obtained also this time.

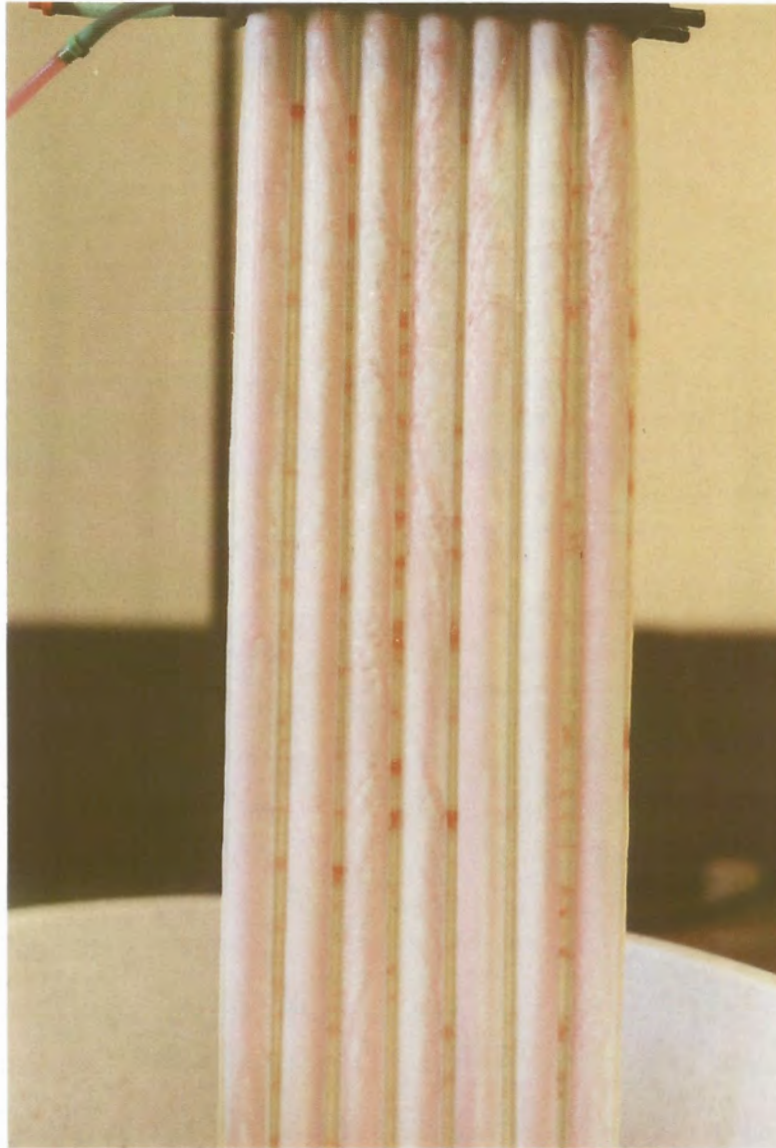


Fig.6.7 Visualization of the streams flowing downwards.

Before the tests with surfactant the plastic film was exposed for many days to dry air instead of being kept in a wet environment. This could have had a negative effect on the treated surface.

We had some indications that additives used in the polypropylene film itself was creating problems with the wettability. Anti-block, slip and other additives often contain waxy low molecular mass oligomers which readily migrate to the surface. Two situations can now arise:

(a) If such migration occurs *before* oxyfluorination (or other surface treatment), then these *mobile* additives (instead of the film itself) are made wettable. As they subsequently move, the surface is no longer wettable.

(b) If a clean surface is oxyfluorinated (or else treated for wettability), then subsequent migration of mobile oligomers (which have low surface energy) to cover the surface will swamp the wettable surface with non-wettable material.

We therefore had film made in a specially formulated grade of high density polyethylene (HDPE) material, containing an absolute minimum of such mobile components/additives. Only the second batch of such film was satisfactory - from the second film blowing company.

Experiments followed with these HDPE films. Before oxyfluorination, some were masked around the weld lines to prevent oxyfluorination in these regions - most with masking tape, others with PVC insulation tape. These films were subjected to three different treatment times - 10, 100 and 1000 seconds. The wettability of the films was tested. In these tests the surfactants were used at a dilution of 10^{-4} . The plastic films were kept always wet in a device built for this purpose. Surprisingly the non-masked films - one shown in figure 6.8 - show better wettability than the masked ones. (Perhaps out-gasses from the tape reacted with the reactive fluorine or oxygen). However, the amount of water flowing down the “furrows”, is (as expected) less in the masked films - but only *slightly* less.

In the non-masked category, the film oxyfluorinated for 1000 seconds shows better wettability than the one treated for 100 seconds. Confirming this trend, the film treated for 10 seconds had the poorest wettability in that category.

In the category of the masked films, the “100 sec” oxyfluorinated film was - surprisingly - better than the one treated for “1000 sec”. This result is not understood. We suspect a labelling error.

In general, the use of surfactants to complement the oxyfluorination process have

enhanced significantly the wettability of water on the plastic films. However, results dependent on surfactants do not seem acceptable for a practical desalinator.

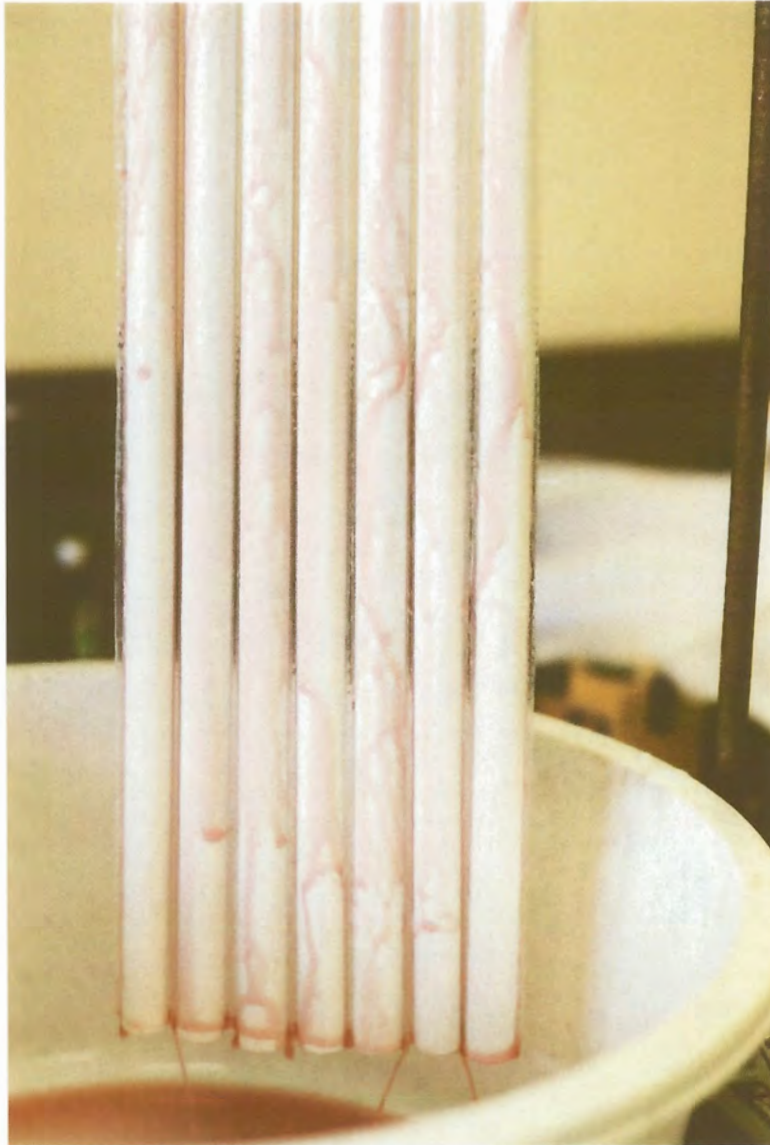


Fig.6.8 View of the flow on a non-masked oxyfluorinated plastic film.

Thus, adjustments of the oxyfluorination conditions were undertaken: - Sets of one and two metre long welded plastic films were sent for oxyfluorination under enhanced treatment conditions (time & concentration of the gas mixture). For the oxyfluorination of plastic films of 2m long, a device was specially built to hold these films equally spaced in spiral layout inside the cylindrical reactor. The testing of the wettability of these oxyfluorinated films was done using the improved setup. There is a limit to what is possible with oxyfluorination, as too high a concentration of these reactive gases causes

melting, carbonisation, or even ignition, of the film. The best obtained results with enhanced conditions were better than before, but still not satisfactory.

It was accidentally found that by slowly “wiping” the inflated tubes with rubber gloves *while water was flowing over the surface*, the wetting of the plastic films improved dramatically. Thus, tests were done to compare the efficiency of about 40 wiping tools of different shapes and materials. The tests indicate that tools with a smooth round contact surface were the most efficient. Whether the wiper material was hydrophilic or hydrophobic made little difference. But *slow* wiping was markedly more efficient than fast.

It appears that the surface treatment - with a very reactive fluorine-oxygen mixture - causes a roughening of the surface. (In a future project atomic force microscope experiments will be done to investigate this hypothesis) It is known [6] that *rough surfaces* show some *hysteresis* effects - *advancing and receding contact angles* for a liquid such as water differ for such surfaces. What happens with *slow* wiping of the air mattresses *with water flowing* against a treated surface, is that *water is dammed* by the smooth wiper against the “air mattress” film. Once wet, as long as water is (even slowly) flowing, the surface remains wetted rather uniformly - in a near ideal manner.

From a practical point of view, the wiping (say once per hour, or per day) may also - like the sponge ball method used in MSF systems - help to remove scale *as it is being formed* (when it is still soft, due to an incomplete crystallization process) [11]. Inside the system, the wipers may also serve as *spacers* between the “air mattresses”. But having a mechanically moving system to wipe each of the thousands (or millions) of tubes inside the vacuum system of a large desalinator, with hot saline water all around, may pose serious problems with the reliability and availability of the system.

With the use of wipers, the problem of the flow along the “furrows” centred on the weld lines still remained a problem, as can be seen in figure 6.9. As mentioned before, different approaches were tried to address that problem. The use of a layer of strongly hydrophobic silicone on the weld lines seems to be the best options so far. The combined action of

wiping the films and using thin layers of silicone on the weld lines improves the wettability significantly. The achievement of complete wettability via oxyfluorination has



Fig. 6.9 Flow dripping through the weld lines of an oxyfluorinated film.

proved unsuccessful after several years' work. Thus, another surface treatment - sulfonation of the specially formulated HDPE film - is in the early stages of being tested. This process uses gaseous sulfur trioxide (SO_3). Figures 6.10 and 6.11 show the first sulfonated films in our wettability test. The brown colour of the films is due to the sulfonation process. At this early stage the first sulfonated films appear to be more wettable than the best oxyfluorinated ones.

6.4 Surface Tension Measurements

Knowledge of the surface tension of a solid is vital for the assessment of its wetting capability by a given liquid. The wetting behaviour of a liquid on a solid surface can be evaluated by measuring the contact angle between the liquid and the solid. Theoretically, a surface is wetted by a liquid if the contact angle between both is less than 90° [6,12].

Complete wettability is achieved if the contact angle is zero degree. It occurs when the surface tension of the solid exceeds that of the liquid.



Fig. 6.10 Sulfonated film with water flowing on its surface.



Fig. 6.11 Another sulfonated film.

When free of oily contamination, all metal heat transfer surfaces used in thin film evaporation (cupro-nickel, titanium, aluminium brass, other aluminium alloys and various grades of stainless steel) are *completely wettable* by water. Clearly, complete wettability plays an important role in achieving a *total wetting* of the evaporating surface - which is essential for efficient and reliable operation of a multi-effect (ME) or vapour compression (VC) desalinators [10]. We consider it also essential for desalinators with polymer heat transfer surfaces. Clearly, an evaporation surface contaminated with oil - or feedwater so contaminated - will not be acceptable for efficient and reliable operation of an ME or VC desalinators.

Table 6.1 lists - for comparison - the surface tension of water and of some polymers.

There are different methods for the determination of the contact angle of a liquid on a given solid surface. The most commonly used methods are sessile drop, captive bubble and the Wilhelmy plate technique. With some methods one can measure only one contact angle (static). This contact angle does not characterise the interaction solid-liquid since solid surfaces are often rough, uneven, and inhomogeneous.

Temperature(°C)	Material	Surface tension (dynes/cm)
25	Water	72
	Sea water	73
25	Polypropylene	30.1
25	Polyethylene	35.7
	Silicones	20 - 26
	Polyamide	46
	PTFE	18

Table 6.1 The surface tension values of some polymeric materials for comparison with that of water.

The Wilhelmy plate method [15] is the technique used in this work. It was chosen because it provides more information about the solid-liquid interaction. Thus, a *contact angle hysteresis* is obtained - the difference between the advancing and the receding

contact angles.

The advancing (maximum) and receding (minimum) angles are automatically calculated by the computer from the force exerted as the sample is dipped into the liquid or withdrawn from it. The equation used by the computer to calculate the dynamic contact angles is:

$$\cos \theta = \frac{F}{\sigma p} \quad (6.1)$$

where F is the insertion/withdrawal force measured by the balance, p the perimeter of the sample in contact with the liquid, σ the surface tension of the liquid probe; and θ the angle formed by the tangent to the point of contact at the solid-liquid-vapour boundaries.

6.4.1 Experimental Setup



Fig.6.12 A DCA series 322 Analyzer.

The instrumentation used for the dynamic contact angle is shown in figure 6.12. It comprises a DCA series 322 Analyzer (from CAHN), a computer, and a printer. The DCA Analyzer includes a microbalance and a movable stage, on which the container with the wetting liquid is placed.

The computer controls the DCA through special software that calculates automatically the contact angles (advancing and receding) and the surface tension.

The samples for the dynamic contact angle measurements, comprising small pieces (30mm x 12.5mm x 39 μ) of plastic film, were thoroughly cleaned. For this, they were introduced into a small container filled with tap water mixed with a commercial surfactant and immersed in an ultrasonic bath for 15min. Thereafter, they were thoroughly rinsed with distilled water and dried. The samples were then introduced into the reactor for oxyfluorination in two sets of five each using oxyfluorination times of 400 and 800s.

The testing of each *sample* started with the measurement of its to be wetted perimeter with a digital vernier caliper. Then it is held vertically suspended by an electro-balance in a fixed position. A container with the probe liquid of known surface tension (e.g. water) is placed on the movable stage. In operation the stage moves up and down at a constant velocity of 40 μ m/s. The sample is immersed into and withdrawn from the liquid. The wetting force on the sample is continuously measured as function of the immersion depth. A printer attached to the apparatus plots the obtained force *versus* depth of immersion, and calculates the advancing and receding contact angles.

The dynamic contact angle hysteresis curve for the samples, subjected to different conditions, is presented in figures 6.13, 6.14 and 6.15. The sample of figure 6.13 had not been surface treated. The results are summarised in table 6.2.

Oxyfluorination time	Dynamic contact angle (degrees)		
	advancing	receding	hysteresis
untreated	84.5	69.9	14.6
400 s	69.2	54.4	14.8
800s	51.8	35.4	16.4

Table 6.2 Dynamic contact angles for PP sample.

As expected in all samples, the advancing contact angles are higher than the receding ones. The contact angle hysteresis increases with the oxyfluorination time. This is under-

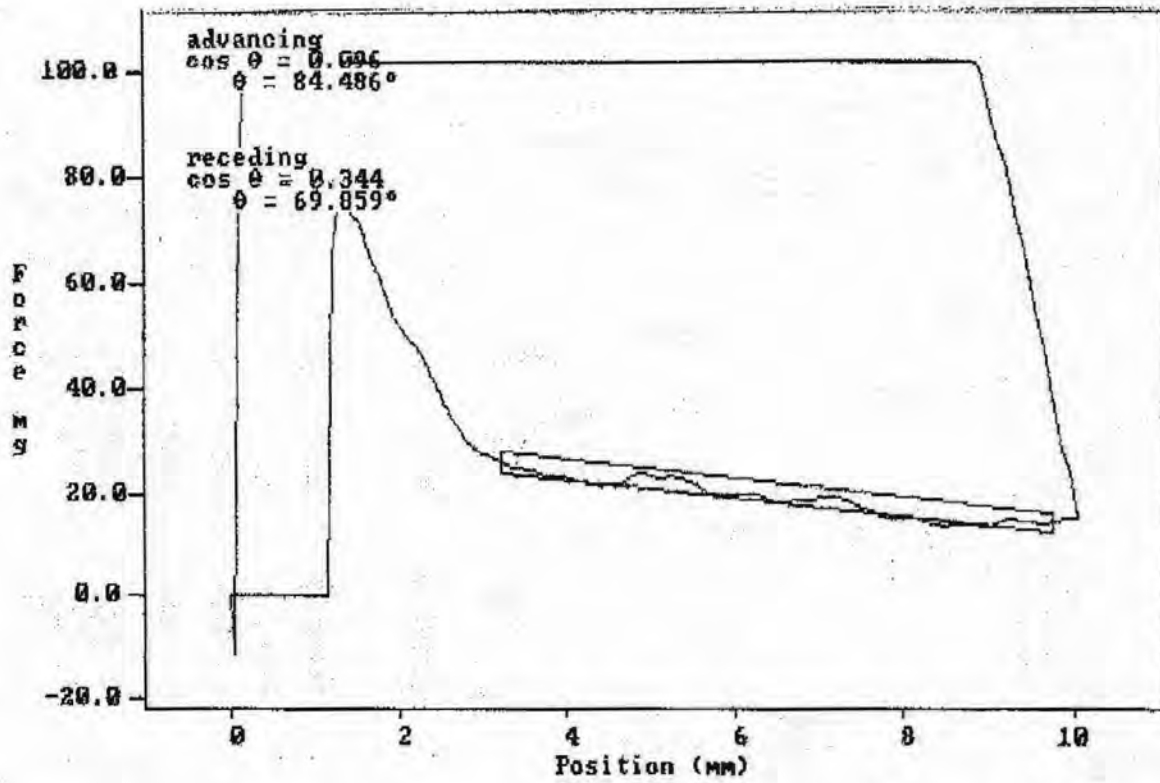


Fig.6.13 Dynamic contact angle hysteresis curve for untreated uniaxially stretched PP film.

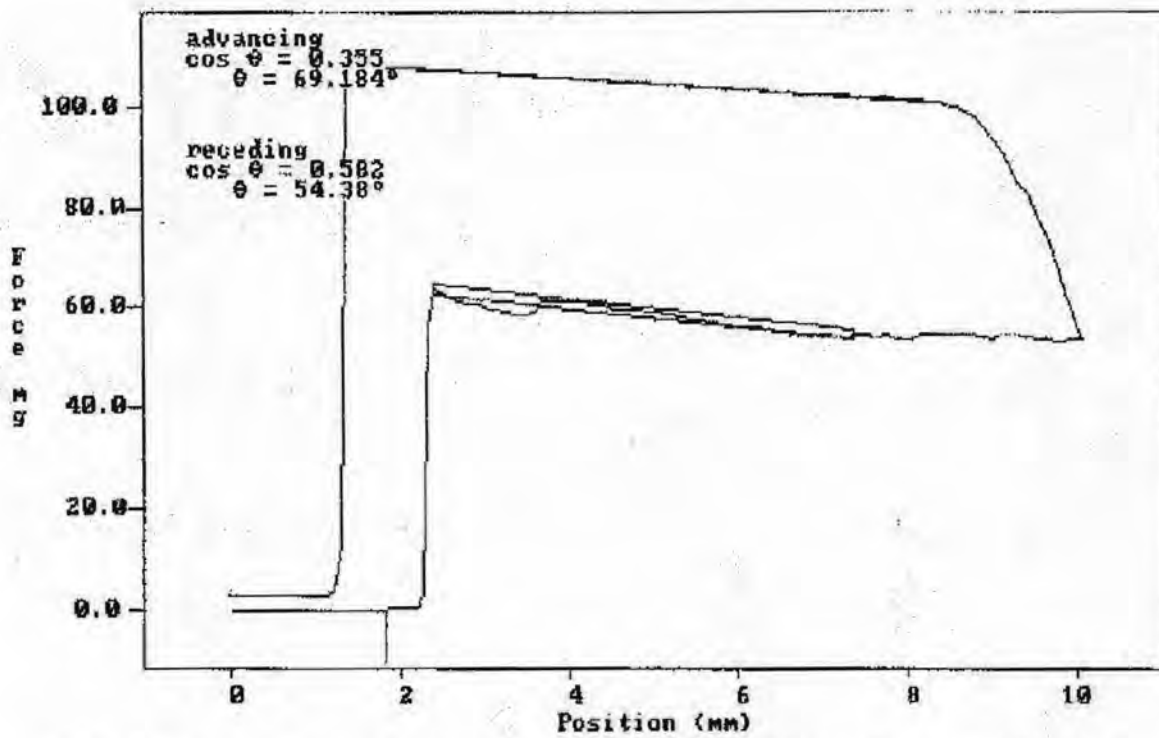


Fig. 6.14 Dynamic contact angle hysteresis curve for a 400s oxyfluorinated PP film.

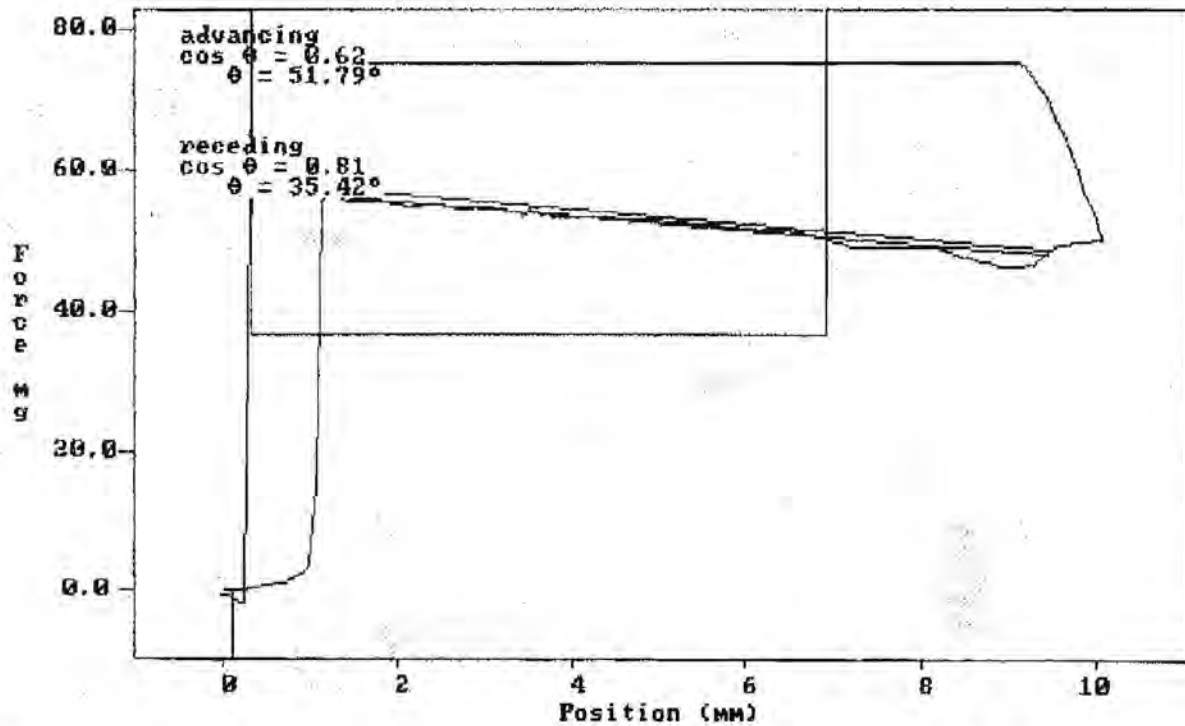


Fig. 6.15 Dynamic contact angle hysteresis curve for a 800s oxyfluorinated PP film.

standable, for the treatment process changes the surface morphology.

The contact angles decreases with the treatment time. With this trend in mind the surface treatment time were increased. However, complete wettability (zero contact angle θ) could not be achieved by oxyfluorination.

6.5 Liquid Distributor

For good heat transfer, an adequate distribution of water (flow mode) onto the outer (evaporation) surface of the thin film “air mattress” heat exchanger element is needed to keep the entire outer surface (except the areas near the weld lines) wet. The distribution of the fluid onto the surface should be even, uniform and at a sufficiently low rate to have film-wise evaporation. The design, construction and materials of the liquid distributor must be such as to avoid or at least minimize the occurrences of blockages.

The following configurations of the liquid distributor were tested:

A) A high density polyethylene (HDPE) distributor tube (5mm ID), with seven holes of one millimetre diameter each, spaced axially 20mm apart. Due to the known ease of

blockage of such small holes, versions with micro-tubes instead of simple hole were tested.

B) A similar HDPE distributor tube with inserted polypropylene (PP) micro-tubes of 1.1 mm inside diameter and 5 mm long: - 7 holes to each side at an angle of 45° from the vertical - to wet “air mattress” elements placed on both sides of the distributor. The tubes facing left are staggered with respect to the ones facing to the right, as the “air mattress” tubes are likewise staggered (see figure 6.16).

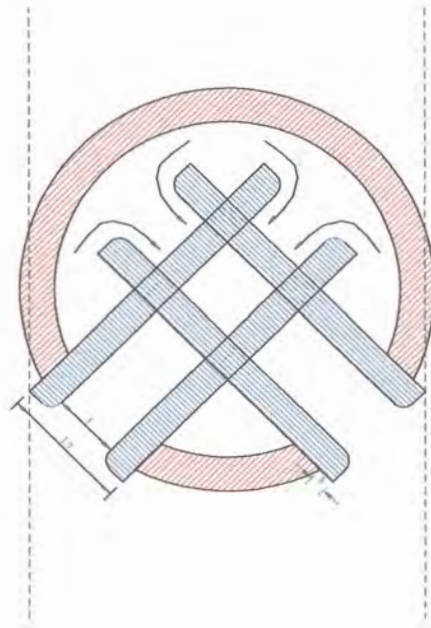


Fig. 6.16 Cross sectional view of the liquid distributor with the inserted micro-tubes.

C) In another setup stainless steel micro-tubes (0.8 mm ID) replaced the PP ones.

For the tests the liquid distributor comprised only one set of micro-tubes all located on the same side of the HDPE plastic tube.

Tests were performed to determine the water head h at which the flow pattern coming from the liquid distributor varies from droplet to jet mode were conducted using the test facility shown in figure 6.17. The setup comprised two basins. The one, usually kept at

fixed height, was used as water source. The other, at the bottom, was used to collect the water discharged from the first basin.



Fig. 6.17 Setup for liquid distributor testing.

The liquid distributor was connected to the top basin through a flexible tube with a tap to interrupt the flow when necessary. The liquid distributor was set at 40 mm below the bottom of the top basin.

A small fountain pump (EDEN 130G) was used to fill the top basin with water to a level sufficient to effect jet mode. With the pump off and the tap open, water from the top basin was released through the liquid distributor into the bottom basin. As the liquid level dropped, the flow pattern varied from jet mode (at the beginning) to jet-droplet mode and

finally to droplet mode. For comparison, with the liquid distributor exhibiting droplet mode the pump was switched on again to refill the top basin and the inverse transitions were observed.

The water levels inside the basin where the changing of flow mode occurs were measured with an ordinary ruler. The corresponding water head h - at the flow distributor - for the three configurations is shown in table 6.3. The values for both directions differ slightly in all configurations, specially in the transition from mixed to droplet mode and vice versa.

Configuration	h (mm)		Observation
	jet \leftrightarrow jet-droplet	jet-droplet \leftrightarrow droplet	
A	124	91	downwards
	126	95	upwards
B	146	63	downwards
	150	70	upwards
C	131	64	downwards
	130	67	upwards

Table 6.3 Water head h for the configurations A, B, and C in the transitions jet - mixed, mixed - droplet, and vice versa.

The determination of the h values for the transition from mixed to droplet mode and vice versa was difficult due to the frequent blockages experienced in the liquid distributors, specially in configuration A.

The holes and the inserted micro-tubes had to be constantly cleaned during the tests. This could have affected the measurements.

As expected the water head h in all configurations reduces from jet via mixed to droplet mode. The factor of reduction is almost equal in configurations B and C. The frequent blockages experienced in configuration A have affected the results in the transition from mixture to droplet mode thus making the reduction factor of A less than that of B and C. Comparatively, configuration A looks more attractive given the low h values in the

transition jet to mixture mode. However, the uncertainty of the reliability of the h values in the other transition makes configuration C a better option.

To establish the nature (laminar, transitional or turbulent) of the flow inside of the distributor the Reynolds number was determined for the three configurations. Transitional flow tends to be unstable - therefore to be avoided. The Reynolds number is given by

$$R_e = \frac{vd_h}{\nu} \quad (6.2)$$

where v is the fluid velocity, ν the kinematic viscosity, and d_h the hydraulic diameter.

The hydraulic diameter - determined for a tube with one inserted micro-tube (see figure 6.16) is given by

$$d_h = \frac{4A_c}{P} \quad (6.3)$$

where A_c is the cross-sectional area for flow and P the wetted perimeter.

The fluid velocity is given by

$$v = \frac{\dot{m}}{\rho A_c} = \frac{\dot{V}}{A_c} \quad (6.4)$$

where \dot{m} is the fluid mass flow rate, ρ the fluid density, and \dot{V} the fluid volume rate.

The average fluid volume rate was obtained by measuring the volume of the fluid collected during 30 seconds in a set of three measurements for each configuration. This was done at the water head where the flow was about to change from jet to mixed mode.

Using the equations (6.2), (6.3) and (6.4) the Reynolds number was calculated by

$$R_e = \frac{\dot{V} d_h}{\nu A_c} \quad (6.5)$$

In the calculation of R_e for configuration A (tube without obstruction), d_h was replaced by the inside tube diameter. The fluid kinematic viscosity ν was evaluated at the temperature of 295K [7].

The obtained values of the Reynolds numbers are shown in table 6.4. The results are far less than the critical value of 2300, where the transition from laminar to turbulent flow inside a round tube normally starts. However, given the existence of obstruction due to the inserted micro-tubes in the configurations B and C, the theoretical critical Reynolds number for similar case is expected to be lower than 2300, since obstruction promotes turbulence.

Configuration	R_e
A	840
B	852
C	440

Table 6.4 Calculated Reynolds numbers for the three configurations with the flow in jet mode.

The calculated Reynolds numbers are nevertheless still far from 2300. Therefore the flow inside the tube in all configurations can be considered as laminar. This is good for the required uniform spreading of the fluid on the plastic film surface.

6.6 Summary

The wettability of the plastic films is essential for the falling film evaporation used in all modern multi-effect and vapour compression desalinators. The surface treatments (oxyfluorination and sulfonation) on the used polymer films did improve their wettability to water. The use of surfactants to complement the surface treatment has enhanced

significantly the wetting of the films. However the results obtained so far are still not satisfactory.

The wiping of the surface of the oxyfluorinated films was another alternative to further improve the wetting of the plastic films. However it appeared to be a complex options to implement in the prototype desalinator, despite the advantages for its use for removing scale and acting as spacers between the “air mattresses”.

To avoid the unwanted capillary action in the space between adjacent film tubes the use of hydrophobic silicone was by far the best solution.

The wettability of the plastic films was quantitatively estimated by determining the contact angles between the liquid (water) and the sample (treated and untreated plastic films) using the Wilhelmy plate technique. The obtained results show a relationship between the oxyfluorination time and the contact angles.

The configurations of the liquid distributor is vital for the desired even, continuous, and uniform spreading of the water on the heat transfer surface to promote falling film evaporation. The use of HDPE plastic tube with inserted metallic micro-tubes appears to be the best solution to avoid undesirable blockages in the liquid distributor.

The flow in all tested liquid distributors' configurations lies inside the laminar region.

6.7 References

1. A. F. Mills, *Heat and Mass Transfer*, Chicago, Irwin 1995.
2. F. P. Incropera and D. P. DeWitt, *Introduction to heat transfer*, New York, Wiley, 1990.
3. A. Bejan , *Heat transfer*, New York, Wiley, 1993.
4. M. Anand, R.E. Cohen, and R.F. Baddour *Surface modification of low density polyethylene in a fluorine gas plasma*, Polymer, 1981 vol. 22.
5. F. J. du Toit and R.D. Sanderson, *Surface fluorination of polypropylene*, 1.

- Characterization of surface properties*, Journal of Fluorine Chemistry 98 (1999) 107 - 114.
6. F. Garbassi, M. Morra, and E. Occiello, *Polymer Surfaces: from Physics to Technology*, Chichester, Wiley, 1996.
 7. Y-H Wei and A.M. Jacobi, *Vapor -shear, geometric, and bundle-depth effects on the intertube falling-film modes*, paper presented at 1st International Conference on the heat Transfer, fluid mechanics, and thermodynamics, Kruger National Park, South Africa, 2002.
 8. J. A. Fox, *An introduction to engineering fluid mechanics*, London, Macmillan, 1974
 9. D. M. Brewis and I. Mathieson, *Adhesion and bonding to polyolefins*, Shawbary, Rapra Technology Ltd, 2002.
 10. V. Baujat and T. Bukato, *Research and development towards the increase of MED units capacity*, proceedings of IDA conference, Paradise Island, Bahamas, 2003.
 11. E. Ghiazza and A.M. Ferro, *The scaling of tubes in MSF Evaporators: A critical review across 20 years of operational experience*, proceedings of IDA conference, Manama, Bahrain, 2002.
 12. Lin Tu, *Development of surface fluorinated polypropylene fibres for use in concrete*, PhD-thesis, Rand Afrikaans University, Johannesburg, 1998.
 13. L. Ramm-Schmidt, H. Eriksson, P. Koistinen, and V. Tiainen, *Liquid distributor for an evaporator*, USA patent 5904807, 1999.
 14. R. Defay and I. Prigogine, *Surface tension and absorption*, London, Longman, 1996.
 15. K. T. Hodgson and J. C. Berg, *Dynamic Wettability Properties of Single Wood Pulp Fibers and their Relationship to Absorbency*, Wood and Fiber Science 20(1) 1988 3 -17

List of Symbols

- A_c : cross-sectional area for flow (m^2)
- d_h : hydraulic diameter (m)
- F : insertion/withdrawal force measured by the balance (N)
- h_e : heat transfer coefficient for evaporation (W/m^2K)
- k : conductivity of polymer film heat transfer material (W/mK)
- \dot{m} : fluid mass flow rate (kg/s)
- p : perimeter of the sample in contact with the liquid (mm)
- P : wetted perimeter (m)
- R_e : Reynolds number
- v : fluid velocity (m/s)
- \dot{V} : fluid volume rate (m^3/s)
- ΔT_o : temperature difference per effect (K or C)
- ΔT_1 : temperature difference for heat transfer between condensing vapour and evaporating saline water In- and outside film tubes (K or C)
- ΔT_e : temperature difference between a heated polymer film surface next to evaporating saline water, and its vapour.
- θ : angle formed by the tangent to the point of contact at the solid-liquid-vapour (degrees)
- ν : kinematic viscosity (m^2/s)
- ρ : fluid density (kg/m^3)
- σ : surface tension of the liquid probe (dynes/cm)